PRAMANA
— journal of
physics

Vol. 69, No. 5
November 2007
pp. 743–748

Photon pairs: Quantum chromodynamics continuum and the Higgs boson

EDMOND L BERGER
High Energy Physics Division, Argonne National Laboratory, Argonne, IL 60439, USA
E-mail: berger@anl.gov

Abstract. A new QCD calculation is summarized for the transverse momentum distribution of photon pairs produced by QCD subprocesses, including all-orders soft-gluon resummation valid at next-to-next-to-leading logarithmic accuracy. Resummation is needed to obtain reliable predictions in the range of transverse momentum where the cross-section is the largest. Results are compared with data from the Fermilab Tevatron and predictions are made for the large hadron collider. The QCD continuum is shown to have a softer spectrum than the Higgs boson signal at the LHC.

Keywords. Higgs; photon pairs; quantum chromodynamics.

PACS Nos 12.15.Ji; 12.38.Cy; 13.85.Qk

1. Introduction

A Higgs boson with mass between 115 and 140 GeV may be identified at hadron colliders through its decay into a pair of energetic photons, a challenging prospect at the Large Hadron Collider in view of the intense background from hadronic production of non-resonant photon pairs. Theoretical predictions of these background processes may be of substantial value in aiding search strategies. Moreover, the perturbative quantum chromodynamics (QCD) calculation of continuum photon-pair production is of theoretical interest in its own right, and data from the Tevatron collider offer an opportunity to test results against experiment.

In this report, I focus on the transverse momentum (Q_{T}) distribution of a pair of photons from both the Higgs boson signal and the QCD continuum. This distribution is important because its behavior affects the precision of the determination of the vertex from which the Higgs boson emerges. Greater activity in Q_{T} associated with Higgs boson production allows a more precise determination of the event vertex. The expected shape of $\mathrm{d}\sigma/\mathrm{d}Q_{\mathrm{T}}$ can affect triggering and analysis strategies. Event modeling, kinematic acceptance, and efficiencies all depend on Q_{T}. Finally, as is shown here, selections on Q_{T} may be useful to enhance the signal to continuum ratio.

A new calculation of the diphoton cross-section in perturbative QCD is presented in ref. [1] and is summarized here. Contributions are included from all perturbative

subprocesses (quark–antiquark, quark–gluon, antiquark–gluon, and gluon–gluon) to next-to-leading order (NLO) accuracy. In addition, to describe properly the behavior of the $Q_{\rm T}$ distribution of the pairs in the region in which $Q_{\rm T} < Q$, where Q is the invariant mass of the photon pair, all-orders resummation of initial-state soft and collinear logarithmic contributions is included, up to next-to-next-to-leading log (NNLL) accuracy. The influence of initial-state gluon radiation on the predicted transverse momentum distributions is evaluated with the Collins–Soper–Sterman (CSS) resummation procedure [2].

Good agreement of our results is obtained with data from the Collider Detector at Fermilab (CDF) collaboration at $p\bar{p}$ collision energy $\sqrt{s} = 1.96$ TeV [3]. We make suggestions for more differential analyses of the data that would allow refined tests of our calculation. Predictions are made for continuum diphoton production at the LHC, and a comparison is presented with the spectrum of photon pairs expected from Higgs boson decay.

2. Analytical calculation

Direct production of continuum photon pairs occurs from $q\bar{q}, \overset{(-)}{q}g$, and gg scattering. NLO perturbative cross-sections (i.e., cross-sections of $\mathcal{O}(\alpha_{\rm s})$ in the $q\bar{q}$ and qg channels, and $\mathcal{O}(\alpha_{\rm s}^3)$ in the gg channel are included as a part of the resummed cross-section. Singular logarithms arise in the NLO cross-sections when the transverse momentum $Q_{\rm T}$ of the $\gamma\gamma$ pair is much smaller than its invariant mass Q. These logarithms are resummed into a Sudakov exponent (composed of two anomalous-dimension functions $A(\mu)$ and $B(\mu)$) and convolutions of the conventional parton densities $f_a(x, \mu_{\rm F})$ with Wilson coefficient functions C. We include the $\mathcal{O}(\alpha_{\rm s}^3)$ expressions for $A(\mu)$, $\mathcal{O}(\alpha_{\rm s}^2)$ expressions for $B(\mu)$, and the C-functions at order $\alpha_{\rm s}$, for all subprocesses. These enhancements elevate the accuracy of the resummed prediction to the NNLL level. The resummed $Q_{\rm T}$ distribution is well-behaved as $Q_{\rm T} \to 0$, unlike its fixed-order counterpart which is singular in this limit.

A full treatment of photon pair production requires that one address the contributions from the quasi-collinear fragmentation of quarks and gluons into photons. Isolation procedures are applied by the experiments to reduce these long-distance contributions, procedures that are only approximately reproducible theoretically. The energy of the hadronic remnants is required to be less than a threshold 'isolation energy' $E_{\rm T}^{\rm iso}$ in a cone $\Delta R = \sqrt{\Delta\eta^2 + \Delta\varphi^2}$ around each photon, with $\Delta\eta$ and $\Delta\varphi$ being the separations of the hadronic remnant(s) from the photon in the plane of pseudo-rapidity η and azimuthal angle φ. The two photons must also be separated in the η–φ plane by an amount exceeding the approximate angular size $\Delta R_{\gamma\gamma}$ of one calorimeter cell. The values of $E_{\rm T}^{\rm iso}$, ΔR, and $\Delta R_{\gamma\gamma}$ serve as crude characteristics of the actual measurement, and the size of the fragmentation contributions depends on the assumed values of these parameters. We find it sufficient in our work to use a simplified fragmentation model to represent the isolated cross-section. We regularize the fragmentation region by imposing a combination of a sharp cut-off $E_{\rm T}^{\rm iso}$ on the transverse energy $E_{\rm T}$ of the final-state quark or gluon and smooth cone isolation [4].

We use two-loop expressions for the running electromagnetic and strong couplings $\alpha(\mu)$ and $\alpha_{\rm s}(\mu)$, as well as the NLO parton distribution function set CTEQ6M [5].

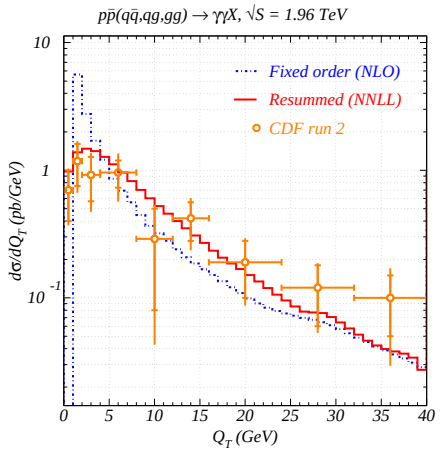

Figure 1. Transverse momentum distributions of diphotons. The dotted histogram shows the result of the next-to-leading order calculation and the solid histogram the result after resummation at NNLL accuracy. The data are from the CDF measurement.

For the renormalization and factorization scales we set $\mu_{\rm R} = \mu_{\rm F} = Q$ in the finite-order perturbative expressions.

3. Comparison with Tevatron data

Our analysis provides the triple-differential cross-section $\mathrm{d}\sigma/\mathrm{d}Q\mathrm{d}Q_{\rm T}\mathrm{d}\Delta\phi$ ($\Delta\phi$ is the difference of the angles of the two photons in the transverse plane). The calculation is especially pertinent for the transverse momentum distribution in the region $Q_{\rm T} \leq Q$, for fixed values of diphoton mass Q. It would be best to compare our multi-differential distribution with experiment, but the collider data tend to be presented in the form of single-differential distributions in Q, $Q_{\rm T}$, and $\Delta\phi$, after integration over the other variables. We follow suit in order to make comparisons with the Tevatron data, but we comment on the features that can be explored if more differential studies are made. For calculations appropriate at Tevatron energies, we impose cuts $|y_\gamma| < 0.9$ on the rapidity of each photon, and $p_{\rm T}^{\gamma} > p_{\rm Tmin}^{\gamma} = 14$ (13) GeV on the transverse momentum of the harder (softer) photon in each $\gamma\gamma$ pair. We choose $E_{\rm T}^{\rm iso} = 1$ GeV, $\Delta R = 0.4$, and $\Delta R_{\gamma\gamma} = 0.3$.

The $Q_{\rm T}$ distribution is shown in figure 1. The NLO calculation displays an unphysical logarithmic singularity as $Q_{\rm T} \to 0$. The result after NNLL resummation is in reasonable agreement with the absolute rate and overall shape of the cross-section. In the two highest-$Q_{\rm T}$ bins, the CDF central values lie above the theory predictions. While the observed excess in this 'shoulder' region is not statistically significant, it has been discussed as a possible indication of enhanced fragmentation contributions in the Tevatron data [3,6].

Our calculations show that most of the shoulder events populate a limited volume of phase space characterized by $\Delta\phi \lesssim 1$ rad, $Q < 27$ GeV, and $Q_{\rm T} \gtrsim 25$ GeV. The location of the shoulder is sensitive to the value of the cut on the minimum

transverse momentum, $p_{\rm T}^{\gamma}$, of the individual photons, moving to larger $Q_{\rm T}$ if these cuts are raised. We note, in addition, that the excess at small $\Delta\phi$ and large $Q_{\rm T}$ is characterized by $Q_{\rm T} \gtrsim Q$.

A new feature of diphoton production, with respect to single photon production, is the prospect that both photons may be produced from fragmentation of the same final-state parton. This fragmentation contribution is expected to be most influential in the region in which both the diphoton invariant mass and the separation $\Delta\phi$ are relatively small, $Q < Q_{\rm T}$ and $\Delta\phi < \pi/4$. From a theoretical point of view, when $Q_{\rm T} > Q$, as in the shoulder region, the calculation must be organized in a different way [7] in order to resum contributions arising from the fragmentation of partons into a pair of photons with small invariant mass. Adequate treatment of the light $\gamma\gamma$ pairs is missing in our calculation and in all other calculations at present. This interesting region warrants further theoretical investigation.

Our theoretical treatment is most reliable in the region in which $Q_{\rm T} < Q$. When the $Q_{\rm T} < Q$ selection is made, the contributions from $\Delta\phi < \pi/2$ are efficiently suppressed, and dependence on tunable isolation parameters and factorization scales is reduced. Our resummed cross-section provides an accurate description of the rate at small values of $Q_{\rm T}$. After the selection $Q_{\rm T} < Q$, we expect that the large $Q_{\rm T}$ shoulder will disappear in the experimental $Q_{\rm T}$ distribution.

Predicted distributions in the invariant mass Q of the photon pair and the separation in $\Delta\phi$ may be found in ref. [1]. An important consequence of the resummation formalism is a logarithmic dependence on the diphoton invariant mass Q. We urge the CDF and D0 collaborations to verify this predicted broadening of the $Q_{\rm T}$ distribution as Q increases.

4. Results for the LHC

To obtain predictions for pp collisions at $\sqrt{s} = 14$ TeV, we require transverse momentum $p_{\rm T}^{\gamma} > 25$ GeV and rapidity $|y_{\gamma}| < 2.5$ for each photon. We impose a somewhat looser isolation restriction than for the Tevatron study, requiring less than $E_{\rm T}^{\rm iso} = 10$ GeV of extra transverse energy inside a cone with $\Delta R = 0.7$ around each photon. Figure 2 shows our resummed transverse momentum distributions for various selections of the diphoton invariant mass at the LHC. The plot shows the predicted broadening of the $Q_{\rm T}$ distribution with increasing mass. Additional predictions for the LHC are presented in ref. [1].

5. Comparison with the Higgs boson signal

Differences arise between the production spectrum for the Higgs boson signal and the QCD continuum. We focus on the dominant gluon fusion mechanism for production of the signal, $gg \to H \to \gamma\gamma$, and we calculate the signal with the same order of precision in the QCD contributions as for the continuum. We include fixed order initial-state QCD corrections at $O(\alpha_{\rm s}^3)$ (NLO) and resummation at NNLL accuracy. These contributions are coded in the same numerical program used to compute the continuum, and we apply the same cuts for both the signal and the continuum. Use of one code minimizes potential deviations than can arise from

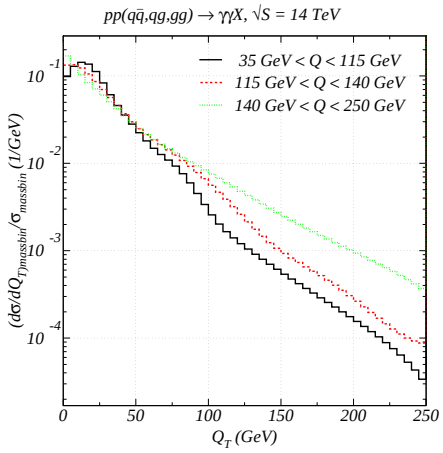

Figure 2. Transverse momentum distributions of diphotons at the LHC for different selections on the invariant mass of the pair of photons.

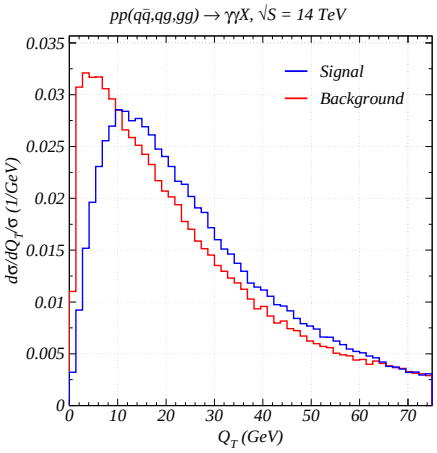

Figure 3. Comparison of the transverse momentum distributions for the Higgs boson signal and diphoton continuum at the LHC, both computed at NNLL accuracy. The continuum is calculated for $128 < Q < 132$ GeV, and the Higgs boson mass is taken to be $m_{\rm H} = 130$ GeV.

codes with different physics content, parton densities, and numerical implementations. We compute the continuum in the range $128 < Q < 132$ GeV and the signal at a fixed Higgs boson mass $m_{\rm H} = 130$ GeV. We use $\mu_{\rm R} = \mu_{\rm F} = Q$ for both the signal and the continuum and the CTEQ6M parton distributions.

The cross-section times branching ratio for the Higgs boson signal is substantially smaller than the continuum. We present distributions normalized to the respective total rates in figure 3. The signal and continuum peak at about 12 and 5 GeV, respectively. The dominant Sudakov exponent $C_{\rm F} = A^{(1)}_{q\bar{q}} = A^{(1)}_{qg}$ that controls gluon radiation for the $q\bar{q}$ and $qg + \bar{q}g$ initial states is less than $A^{(1)}_{gg} = C_A$ that controls the gg case. More gluon radiation in the gg case explains the broader $Q_{\rm T}$ spectrum for the Higgs boson signal. The comparison in figure 3 suggests that the signal-to-background ratio would be enhanced if a cut is made to restrict $Q_{\rm T} > 10$ GeV. Additional differences between the signal and continuum are shown in ref. [1], including the rapidity difference of the two photons [8], the scattering angle in the Collins–Soper frame $\tanh((y^\gamma_1 - y^\gamma_2)/2) = \cos\theta^*$, and the difference between the azimuthal angles of the photons.

6. Summary

A new QCD calculation is presented of the transverse momentum distribution of photon pairs produced at hadron colliders, including all-orders resummation of initial-state soft-gluon radiation valid at next-to-next-to-leading logarithmic accuracy. This calculation is most appropriate for values of $\gamma\gamma$ transverse momentum

$Q_{\rm T}$ not in excess of the $\gamma\gamma$ invariant mass Q. Resummation changes both the shape and normalization of the $Q_{\rm T}$ distribution, with respect to a finite-order calculation, in the range of values of $Q_{\rm T}$ where the cross-section is largest. Comparison of our results with data from the Fermilab Tevatron shows good agreement, and we offer suggestions for a more differential analysis of the Tevatron data. We also include predictions for the Large Hadron Collider.

Acknowledgments

This work is based on a collaboration with Csaba Balazs and Pavel Nadolsky at Argonne and with Chien-Peng Yuan of Michigan State University. Work at Argonne is supported in part by the U.S. Department of Energy, Division of High Energy Physics, Contract W-31-109-ENG-38.

References

[1] C Balazs, E L Berger, P Nadolsky and C P Yuan, *Phys. Lett.* **B637**, 235, (2006), arXiv:hep-ph/0603037; *Phys. Rev.* **D76**, 013008 (2007), arXiv:hep-ph/0702003; *Phys. Rev.* **D76**, 013009 (2007), arXiv:0704.001 [hep-ph]
[2] J C Collins, D E Soper and G Sterman, *Nucl. Phys.* **B250**, 199 (1985)
[3] CDF Collaboration: D Acosta, *et al*, *Phys. Rev. Lett.* **95**, 022003 (2005)
[4] S Frixione, *Phys. Lett.* **B429**, 369 (1998)
[5] J Pumplin *et al*, *J. High Energy Phys.* **07**, 012 (2002)
[6] T Binoth, J-P Guillet, E Pilon and M Werlen, *Phys. Rev.* **D63**, 114016 (2001)
[7] E L Berger, L E Gordon and M Klasen, *Phys. Rev.* **D58**, 074012 (1998)
E L Berger, J Qiu and X Zhang, *Phys. Rev.* **D65**, 034006 (2002)
[8] Z Bern, L J Dixon and C R Schmidt, *Phys. Rev.* **D66**, 074018 (2002)